Journal of Pharmaceutical and Biomedical Analysis 50 (2009) 803–808

Contents lists available at ScienceDirect

Journal of Pharmaceutical and Biomedical Analysis

journal homepage: www.elsevier.com/locate/jpba

Determination of free amino acid content in Radix *Pseudostellariae* using near infrared (NIR) spectroscopy and different multivariate calibrations

Hao Lin, Quansheng Chen*, Jiewen Zhao*, Ping Zhou

School of Food & Biological Engineering, Jiangsu University, Xuefu Road 301#, Jiangsu, 212013 Zhenjiang, PR China

ARTICLE INFO

Article history:
Received 23 March 2009
Received in revised form 19 June 2009
Accepted 19 June 2009
Available online 27 June 2009

Keywords:
Radix *Pseudostellariae*
Free amino acid content
Near infrared (NIR) spectroscopy
Multivariate calibration

ABSTRACT

Near infrared (NIR) spectroscopy combined with multivariate calibration was attempted to analyze free amino acid content of Radix *Pseudostellariae*. The original spectra of *Pseudostellariae* samples in wavelength range of 10000–4000 cm^{-1} were acquired. Partial least squares (PLS), kernel PLS (k-PLS), back propagation neural network (BP-NN), and support vector regression (SVR) algorithms were performed comparatively to develop calibration models. Some parameters of the calibration models were optimized by cross-validation. The performance of BP-NN model was better than PLS, k-PLS, and SVR models. The root mean square error of prediction (RMSEP) and the correlation coefficient (*R*) of BP-NN model were 0.687 and 0.889 in prediction set respectively. Results showed that NIR spectroscopy combined with multivariate calibration has significant potential in quantitative analysis of free amino acid content in Radix *Pseudostellariae*.

1. Introduction

Pseudostellariae (viz. Taizishen in Chinese) as a well known traditional Chinese medicinal herb (TMC) has a sweet and slightly bitter taste. The dried root, defined as 'Radix *pseudostellariae*', has various drug activities. Studies have proved out its multiple pharmacological effects such as anti-oxidation, anti-depressant, anti-fatigue and promoting the immune system, etc. [1]. *Pseudostellariae* is distributed widely in China. However, the quality and efficacy of same species are somewhat jagged according to different cultivated area with the disparity of growing conditions such as soil and climate.

In the past two decades, some studies had revealed that Radix *Pseudostellariae* contained a variety of chemical ingredients, which are some beneficial medicinal properties [2]. Among them, free amino acid is very important. The content of free amino acid is often considered as an important quality index of Radix *pseudostellariae*. Most currently available are techniques restricted to a few chemical analysis tools such as high performance liquid chromatography (HPLC), gas chromatographic (GC), ultraviolet (UV) spectrometry [3]. These methods are precise, but all destructive, time-consuming and costly. Therefore, a rapid and non-destructive analytical method is essentially required.

Near-infrared (NIR) spectroscopy is a fast, accurate and non-destructive technique, and it has been proved to be a powerful analytical tool used in many fields [4–9]. In recent years, NIR combined with pattern recognition techniques, has attracted considerable attention in discrimination of similar biological materials, such as tea [10], fruit [11], polysulfone membranes [12] and Chinese herbs [13,14]. NIR spectroscopy also shows promising ability for chemical content analysis [15–17]. However, few studies have been reported on the determination of chemical content in Radix *pseudostellariae* using NIR spectroscopy.

In this work, the content of free amino acid in Radix *Pseudostellariae* samples was analyzed by NIR spectroscopy combined with multivariate calibrations. To compare calibration models, the algorithms of partial least squares (PLS), kernel PLS (k-PLS), back propagation neural network (BP-NN), and support vector regression (SVR) were performed. These models were optimized according to cross-validation, and the root mean square error of prediction (RMSEP) and the correlation coefficient (*R*) in prediction set were used to evaluate them.

2. Materials and methods

2.1. Sample preparation

All Radix *Pseudostellariae* samples in the experiments were acquired from five different geographical regions of PR China ('Anhui' province, 'Guizhou' province, 'Henan' province, 'Jiangsu' province, 'Fujian' province), and belong to the same species. Before data acquisition, all samples were dried in a forced-draught oven (Shanghai Yi-Heng Machine Co. Shanghai, China) at 105 °C for about 5 h to remove moisture from them. After being cleaned through

* Corresponding authors. Tel.: +86 511 8790308; fax: +86 511 8780201.
E-mail addresses: q.s.chen@hotmail.com (Q. Chen), zhao.jiewen@ujs.edu.cn (J. Zhao).

0731-7085/$ – see front matter © 2009 Elsevier B.V. All rights reserved.
doi:10.1016/j.jpba.2009.06.040

brushing soil off the surface, the samples were crushed into powder by a cyclone mill for consistent measuring. The particle size of powder was controlled below 80 meshes, then put the sieved in airtight jars for further analysis.

2.2. NIR spectroscopy measurement

Antaris II Near-infrared spectrophotometer (Thermo Electron Co., USA) with an integrating sphere was used to collect the NIR spectra in reflectance mode. Each spectrum was the average of 32 scanning spectra. The range of spectra was from 10000 cm^{-1} to 4000 cm^{-1}, and the data were measured in 1.928 cm^{-1} intervals, which resulted in 3112 variables.

A standard sample cup specifically designed by Thermo Electron Co. was used for performing the Radix *Pseudostellariae* spectra collection. For each sample, approximately 1 g of dry Radix *Pseudostellariae* powder was packed into the sample cup. Each sample was collected three times, and the average of the three spectra was used as original information for following analysis. The temperature was kept around 25 °C and the humidity was kept at a steady level in the laboratory.

2.3. Spectral data processing

Fig. 1a shows NIR spectra of Radix *Pseudostellariae* samples from five different origins. NIR spectra could be affected by the physical properties of the samples and other environmental noises. Thus, it is necessary to perform mathematical processing to reduce the systematic noise, and enhance the contribution of the chemical composition. In this study, several spectral preprocessing methods were applied comparatively. These methods are standard normal variate transformation (SNV), multiplicative scatter correction (MSC), first derivative and second derivative. SNV is a mathematical transformation method used to remove slope variation and correct scatter effects in spectra. Each spectrum is corrected individually by first centering the spectral values, and then the centered spectrum is scaled by the standard deviation calculated from the individual spectral values. MSC is another important procedure for the correction of scatter light. It is used to modify the additive and multiplicative effects in the spectra on the basis of different particle sizes. The technique is also applied to correct for additive and multiplicative effects in the spectra. First and second derivatives focus on eliminating baseline drifts and enhancing small spectral differences [18].

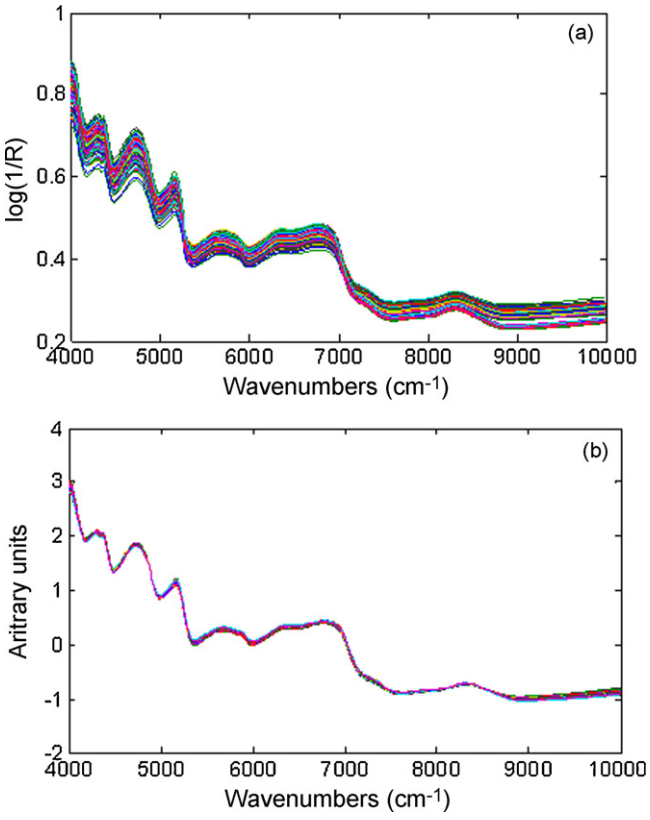

Fig. 1. Raw spectra of samples (a), and after SNV preprocessing (b).

Comparing with these preprocessing methods, SNV method was as good as MSC, better than first and second derivatives. The reason was that dry Radix *Pseudostellariae* particle solid was easy to bring in scatter light. SNV and MSC spectral preprocessing methods have better ability in correcting light scatter, and can also remove slope variation [19,20]. Therefore, SNV preprocessing method was applied in this work, and NIR spectral after SNV preprocessing is presented in Fig. 1b.

2.4. Active components content

The reference content of free amino acid content was reference measured by a ninhydrin color [21]. An UV-2401 spectrophotometer (Shimadzu Corporation, Japan) was used to detect the absorbance (E) of the reaction solution in a 1 cm light-path cell at 570 nm. The calibration standard is pyrrolidinecarboxylic acid.

2.5. Software

All algorithms were implemented in Matlab V7.1 (Mathworks, USA) under Windows XP. Result Software (Antaris II System, Thermo Electron Co., USA) was used in NIR spectral data acquisition. SVM Matlab codes were downloaded free of charge from http://www.esat.kuleuven.ac.be/sista/lssvmlab/.

3. Results and discussion

3.1. Calibration models

In this work, 85 samples from five different geographical origins were investigated, and each geographical origin has 17 samples. All 85 samples were divided into two subsets. One of it called calibration set was used to build model, and the other called prediction set was used to test the robustness of model. To avoid bias in subset division, all samples had been sorted according to their respective y-value (viz. the reference measurement value of free amino acid content). One of every three samples was divided into the prediction set. Finally, the calibration set contained 57 spectra; the remaining 28 spectra constituted the prediction set. As shown in Table 1, the range of y-value in calibration set covered the range in the prediction set. Therefore the distribution of the samples is appropriate in calibration and prediction set.

Table 1
Reference measurement of free amino acid content in calibration and prediction sets.

Subsets	Units (%)	S.N.	Range	Mean	S.D.
Calibration set	g/g	57	7.42–0.58	4.54	1.91
Prediction set	g/g	28	6.35–0.94	4.47	1.68

S.N., sample number; S.D., standard deviation.

The performance of the final model was evaluated according to three types of number, the root mean square error of cross-validation (RMSECV), the root mean square error of prediction and the correlation coefficient [22]. For RMSECV, a leave-one-sample-

out cross-validation was performed: the spectrum of one sample in the calibration set was left out from this set, and a model was built with the remaining spectra of the calibration set. The RMSECV was then calculated with following relation:

$$\mathrm{RMSECV} = \sqrt{\frac{\sum_{i=1}^{n}(\hat{y}_{\setminus i} - y_i)^2}{n}} \quad (1)$$

where n is the number of samples in the calibration set, y_i is the reference measurement result for sample i, and $\hat{y}_{\setminus i}$ is the estimated result for sample i when the model is constructed with sample i removed. The number of factors included in the model was chosen according to the lowest RMSECV. This procedure was repeated for each of the preprocessed spectra. In the prediction set, the RMSEP was calculated as follows:

$$\mathrm{RMSEP} = \sqrt{\frac{\sum_{i=1}^{n}(y_i - \hat{y}_i)^2}{n}} \quad (2)$$

where n is the number of samples in the prediction set, y_i is the reference measurement result for prediction sample i, and $\hat{y}_i$ is the estimated result of the model for prediction sample i.

Finally the optimal model was chosen according to the overall lowest RMSECV. Correlation coefficients between the predicted and the measured value were calculated for both the calibration and the prediction sets, using Eq. (3), where $\bar{y}$ is the mean of the references measurements results.

$$R = \sqrt{1 - \frac{\sum_{i=1}^{n}(\hat{y}_i - y_i)^2}{\sum_{i=1}^{n}(\hat{y}_i - \bar{y})^2}} \quad (3)$$

3.2. PLS model

PLS analysis could consider simultaneously the variable matrix Y (the physiological properties of interest) and the variable matrix X (the spectral data) [23]. It can establish a regression model to predict the content of chemical components or responses to the Y-value. So it is widely implied in NIR spectroscopy analysis [24]. To reduce the dimensionality and compress the original spectral data, the principal components (PCs) obtained from principle component analysis (PCA) were considered as new eigenvectors of the original spectra. In the development of PLS model, full cross-validation was used to evaluate the quality and prevent over fitting of calibration model. The number of PLS components (i.e., PCs) can affect the performance of PLS model, and it should be optimized by cross-validation in model calibration. The optimal number of PLS components is corresponding to the lowest RMSECV value.

Fig. 2a shows the RMSECV values of PLS model under different PCs by cross-validation. When using 9 PCs, the lowest RMSECV could be achieved, and the corresponding PLS model was the optimal model. The RMSEP and the R of PLS model were 0.969 and 0.8075 in prediction set respectively.

3.3. Kernel PLS model

Considering PLS, a linear calibration method, may not provide a complete solution to the problem. So, k-PLS, a non-linear approach was also attempted in this work. The main feature of k-PLS is that the scores and loadings are calculated from the so-called kernel matrix rather than from the original data matrix [25]. This algorithm allows the PLS calibration to be carried out in a space of nonlinearly transformed input data—the so-called feature space [26]. The details of k-PLS algorithm could be found in the literature [27].

It has been demonstrated that RBF kernel can give a good performance under general smoothness assumptions [25]. In this work, RBF kernel with 1 order was used to build calibration model. As PLS model, the optimal number of k-PLS components is corresponding to the lowest RMSECV value by cross-validation in calibration model. Fig. 2b shows the RMSECV values of k-PLS model under different PCs by cross-validation. When using 5 PCs, the lowest RMSECV could be obtained, and the corresponding k-PLS model was the optimal model. Here, the value of RMSEP was 0.828, and R was 0.838 in prediction set.

3.4. BP-NN model

Back propagation neural network is a powerful data-modeling tool to capture and represent complex relationships between inputs and outputs. The eigenvectors (PCs) obtained from PCA are processed by the neural network. The output expressed the resemblance that an object corresponds with a training pattern. Along with every pass of a training pattern and adjustment of the weight factors, the network output error will gradually become less until it meets the desired value. One cycle through all the training patterns is an epoch. Before the optimal accordance of the network output error is achieved for all training patterns, numbers of epochs are required for the back propagation [28–30].

In this work, BP-NN as one of the calibration methods for comparison was applied. Three layers (i.e., an input layer, a hidden layers and an output layer) of BP-NN were arranged. The number of PCs was also optimized according to cross-validation in this work, and the optimal PCs determined according with lowest RMSECV value was used as input layers. The output of BP-NN was the free amino acid content of interest. The hidden nodes were optimized by 'trial and error' [31], and optimal of hidden nodes is evaluated by the

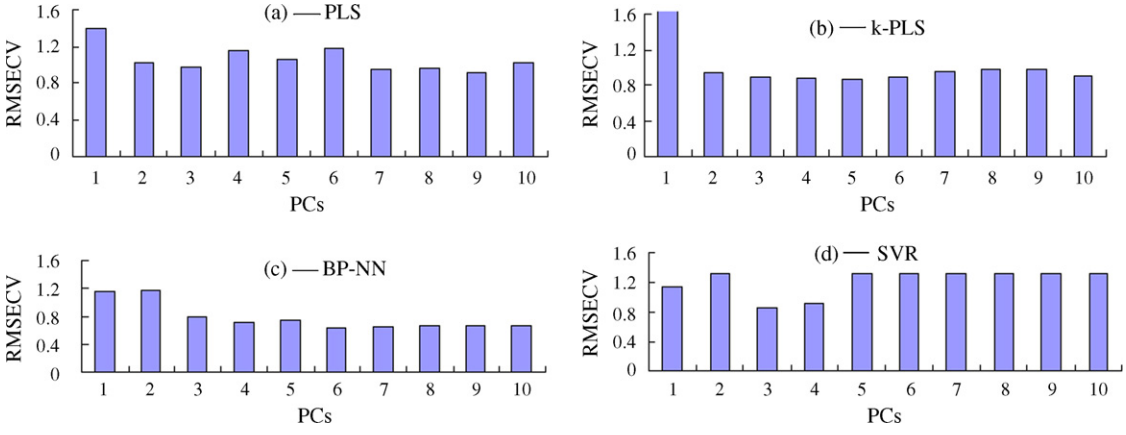

Fig. 2. RMSECV values of four calibration models under different PCs.

minimal mean square error (MSE) value [32]. The learning rate factor and momentum factor were all set to 0.1; the initial weights were 0.3; scale function used was the 'tan *h*' function. The permitted regression error was set as 0.01 and the maximal time of training was 2000. When 6 PCs and 8 hidden layers were selected, the optimal performance can be achieved. Finally, the optimum network architecture was obtained with topological architecture 6-8-1.

Fig. 2c shows the RMSECV values of BP-NN model under different PCs by cross-validation. When 6 PCs were used, the lowest RMSECV could be achieved, and the corresponding BP-NN model was the optimal model. Here, the value of RMSEP was 0.687, and *R* was 0.889 in prediction set.

3.5. SVR model

Support vector machine (SVM) is typically adopted to describe classification problems with support vector methods [33]. However, with the introduction of ε-insensitive loss function, SVM has been extended to solve nonlinear regression estimation problems, and a regression version of SVM is also called support vector regression [34]. The basic concept of SVR is mapping the nonlinearly the original data x into a higher dimensional feature space. So it turns to solve a linear regression problem in this feature space. The transformation into higher dimensional space is implemented by a kernel function [35]. In general, there are three classical kernel functions: polynomial kernel function, RBF kernel function, and sigmoid kernel function. Selection of kernel function has a high influence on the performance of SVR. Comparing with other feasible kernel functions, RBF could handle the linear and nonlinear relationships between the spectra and target attributes. Besides, RBF is able to reduce the computational complexity of the training procedure and give a good performance under general smoothness assumptions [36,37]. Thus, the kernel function of SVR in this work was RBF.

Just as other calibration models, the optimal PCs of SVR was also determined according to the lowest RMSECV values. Fig. 2d shows the RMSECV values of SVR model under different PCs by cross-validation. When 3 PCs were used, the lowest RMSECV could be achieved, and the corresponding SVR model was the optimal model.

In order to obtain a good performance, the regularization parameter C and parameter σ of the kernel function in SVR model have to be optimized. Parameter C determines the trade-off between minimizing the training error and minimizing model complexity. Parameter σ implicitly defines the non-linear mapping from input space to some high-dimensional feature space [38].

Before the parameters were optimized, an initial value was set, the range of parameters optimization was based on the initial value setting. Cross-validation in the calibration set was used to direct the optimization process. As shown in Fig. 3, the search procedure was carried out in two search steps. First, a comparatively large step length in a 10×10 grid represented as "·" was applied. Subsequently, a much smaller step length was used to obtain the optimal combination of these parameters, and the search grid "×" was also shown in Fig. 3. The optimal search area is determined based on last step. The optimal C and σ^2 for calibration models was found at the value of 157.15 and 0.74, respectively. Here, the value of RMSEP was 0.7312 and the value of R was 0.8711 in prediction set.

3.6. Comparison of four calibration methods

Four multivariate calibration methods, PLS, K-PLS, BP-NN and SVR, were investigated in this work. Table 2 shows the compared results in prediction set from the four models. These results implied that it was feasible to analyze free amino acid content in *Pseudostellariae* by NIR spectroscopy. According to investigation of the results from four models, k-PLS, BP-NN and SVR models have a better performance than PLS model. The scatter plot of references measured and NIR predicted by four calibration models in prediction set were shown in Fig. 4. It could be explained that k-PLS, BP-NN and SVR are intended to be universal non-linear approximators. PLS, on the other hand, is a linear method, although it may handle mild non-linearities by including extra latent variables into the model. Free amino acid in radix *Pseudostellariae* is a mixture contains a variety of amino acid compositions [39]. The NIR bands are composed of overtones and combinations of fundamental vibrations of corresponding organic groups from the mid-infrared. Therefore, the relationship between the NIR spectra and free amino acid content maybe complicated which is more inclined to non-linear rather than linear. Furthermore, the approach of augmented partial residual plots (APARPs) was used to detect the relationship between the NIR spectra and free amino acid content [40]. A quantitative numerical tool (run test) was employed to calculate the non-linearity based on APARPs methods, and the z-value is 4.614 exceeding the critical value ($|z| = 1.96$). So, a non-linearity conclusion is credible, and moving from PLS to non-linear methods is reasonable. It can also be explained by some relevant statistical learning theories. In generally, non-linear method is stronger than linear method in the level of self-learning and self-adjust. The results indicated that the latent nonlinear information was helpful to improve the prediction performance of model.

Investigated between k-PLS, BP-NN and SVR, BP-NN model got better performance than the other algorithms. It can be conclude that the topological network architecture of BP-NN may be more suitable for the analysis of complicated chemical component of free amino acid in radix *Pseudostellariae*. Generally, the prediction of activities is a main objective of the quantitative structure activity relationships (QSAR) [41]. ANN has proven to be an excellent approach among QSAR studies [42,43]. Therefore, BP-NN model achieved a better result in the prediction of free amino acid content in radix *Pseudostellariae*.

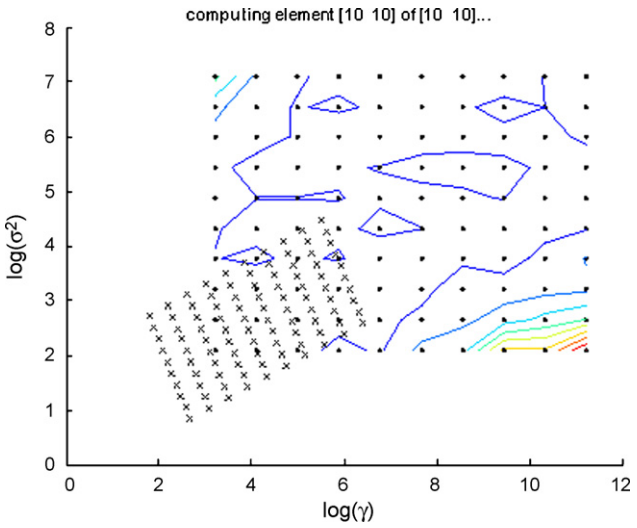

Fig. 3. Contour plot of the optimization the parameters C and σ^2 in the calibration set.

Table 2
Comparison of the results from four multivariate calibration models.

Model	PCs	Prediction set	
		RMSEP	*R*
PLS	9	0.969	0.8075
K-PLS	5	0.828	0.838
BP-NN	6	0.687	0.889
SVR	3	0.7312	0.8711

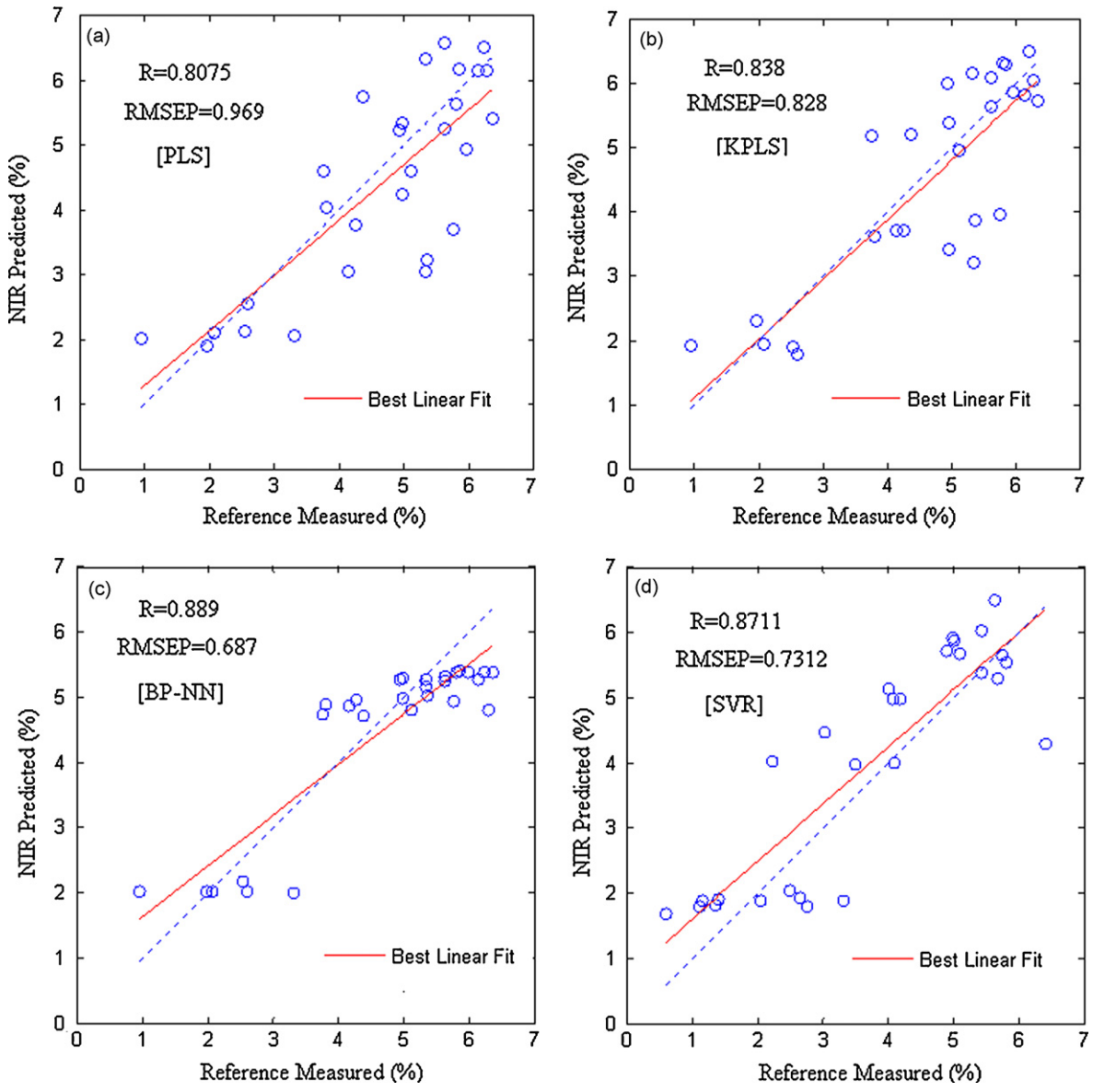

Fig. 4. Reference measured versus NIR predicted by different multivariate calibration models in prediction set.

4. Conclusion

The overall results showed that free amino acid content in Radix *Pseudostellariae* can be analyzed by NIR spectroscopy coupled with multivariate calibration models. BP-NN model showed great potential in quantitative structure activity relationships study for its topological network architecture. The optimal performance was achieved when BP-NN model was used and with $R = 0.889$ and RMSEP = 0.687 in prediction set. These results suggested NIR spectroscopy may have commercial and regulatory potential to avoid time-consuming work, costly and laborious chemical analysis. Further studies will be developed at examining the feasibility of NIR spectroscopy to discriminate mixed species of Radix *Pseudostellariae* or other herbal medicines.

Acknowledgements

This work has been financially supported by the National Natural Science Foundation of PR China (Grant No. 30800666) and the National High Technology Research and Development Program of China (863 Project, No. 2006AA10Z263). We are grateful to the website http://www.esat.kuleuven.ac.be/sista/lssvmlab/, where we downloaded SVM Matlab codes free of charge.

References

[1] X.Q. Xu, Q.L. Li, J.D. Yuan, Chin. J. Anal. Chem. 35 (2007) 206–210.
[2] Y.Y. Chen, Y. Ding, W. Wang, Tsinghua Sci. Technol. 12 (2007) 389–393.
[3] J. Zhang, Y.B. Li, D.W. Wang, Z.Q. Yin, J.A. Chin, J. Mater. Med. 32 (2007) 1051–1053.
[4] Y.A. Wu, H.J. Kim, J.H. Cho, J. Pharmaceut. Biomed. Anal. 21 (1999) 407–413.
[5] Y.A. Wu, C.H. Cho, H.J. Kim, Microchem. J. 73 (2002) 299–306.
[6] L. Wang, F.S.C. Lee, X.R. Wang, Y. He, LWT 40 (2007) 83–88.
[7] X.B. Huang, H.Y. Yu, H.R. Xu, J. Food Eng. 87 (2008) 303–313.
[8] O. Jirsa, M. Hrušková, I. Švec, J. Food Eng. 87 (2008) 21–25.
[9] M.B. Roman, Z.S. Raviya, Fuel 87 (2008) 1096–1101.
[10] J.W. Zhao, Q.S. Chen, X.Y. Huang, C.H. Fang, J. Pharmaceut. Biomed. Anal. 41 (2006) 1198–1204.
[11] J.A. Cayuela, Postharvest Biol. Technol. 47 (2008) 75–80.
[12] A. Conesa, T. Gumí, J. Coello, C. Palet, J. Membrane Sci. 300 (2007) 122–130.
[13] Y.A. Wu, H.J. Kim, J.H. Cho, Microchem. J. 63 (1999) 61–70.
[14] Y. Chen, M.M. Xie, Y. Yan, Anal. Chim. Acta 618 (2008) 121–130.
[15] F. Liu, F. Zhang, Z.L. Jin, Y. He, H. Fang, Q.F. Ye, W.J. Zhou, Anal. Chim. Acta 629 (2008) 56–65.
[16] N. Qu, M.C. Zhu, H. Mi, Y. Dou, Y.L. Ren, Spectrochim. Acta A: Mol. Biol. 70 (2008) 1146–1151.
[17] C. Ravna, E. Skibsted, R. Bro, J. Pharmaceut. Biomed. Anal. 48 (2008) 554–561.

[18] A.S. Barros, R. Pinto, D.J.R. Bouveresse, D.N. Rutledge, Chemometr. Intell. Lab. Syst. 93 (2008) 43–48.
[19] V. Kestens, J. Charoud-Got, A. Bau, A. Bernreuther, H. Emteborg, Food Chem. 106 (2008) 1359–1365.
[20] R. Font, M.D. Río-Celestino, E. Cartea, A.D. Haro-Bailón, Phytochemistry 66 (2005) 175–185.
[21] X.B. Zou, J.W. Zhao, X.Y. Huang, Y.X. Li, Chemometr. Intell. Lab. Syst. 87 (2007) 43–51.
[22] X.H. Liu, Y.M. Kan, Y.U. Xiang, Y.X. Wang, Nanjing University of TMC 3 (1993) 42–44.
[23] R.M. Balabin, R.Z. Safieva, E.I. Lomakina, Chemometr. Intell. Lab. Syst. 88 (2007) 183–188.
[24] V. Thomas, S. Robert, J. Richard, Chemometr. Intell. Lab. Syst. 90 (2008) 8–14.
[25] B.M. Nicolaï, K.I. Theron, J. Lammertyn, Chemometr. Intell. Lab. Syst. 85 (2007) 243–252.
[26] K. Kim, J.M. Lee, I.B. Lee, Chemometr. Intell. Lab. Syst. 79 (2005) 22–30.
[27] R. Rosipal, L.J. Trejo, J. Mach. Learn. Res. 2 (2001) 97–123.
[28] K. Yetilmezsoy, S. Demirel, J. Hazard. Mater. 153 (2008) 1288–1300.
[29] M. O'Farrell, E. Lewisa, C. Flanagana, W.B. Lyonsa, N. Jackmanb, Sensor Actuator B: Chem. 107 (2005) 104–112.
[30] N. Caglar, M. Elmas, Z.D. Yaman, M. Saribiyik, Const. Build. Mater. 22 (2008) 788–800.
[31] C.A. Emilio, J.F. Magallanes, M.I. Litter, Anal. Chim. Acta 595 (2007) 89–97.
[32] X.L. Li, Y. He, Biosyst. Eng. 99 (2008) 313–332.
[33] F. Chauchard, R. Cogdill, S. Roussel, J.M. Roger, V. Bellon-Maurel, Chemometr. Intell. Lab. Syst. 71 (2004) 141–150.
[34] S.F. Fang, M.P. Wang, W.H. Qi, F. Zheng, Comput. Mater. Sci. 44 (2008) 647–655.
[35] U. Thissen, M. Pepers, B. Üstűn, W.J. Melssen, L.M.C. Buydens, Chemometr. Intell. Lab. Syst. 73 (2004) 169–179.
[36] J.A. Fernández Pierna, V. Baeten, P. Dardenne, Chemometr. Intell. Lab. Syst. 84 (2006) 114–118.
[37] N. Labbé, S.H. Lee, H.W. Cho, M.K. Jeong, N. André, Bioresour. Technol. 99 (2008) 8445–8452.
[38] Q.S. Chen, J.W. Zhao, C.H. Fang, D.M. Wang, Spectrochim. Acta A: Mol. Biol. 66 (2007) 568–574.
[39] G.D. Yu, X.P. Liu, H.J. Pan, Chin. Wild Plant Resour. 18 (1999) 9–11.
[40] V. Centner, O.E. de Noord, D.L. Massart, Anal. Chim. Acta 376 (1998) 153–168.
[41] S.Y. Tham, S. Agatonovic-Kustrina, J. Pharmaceut. Biomed. Anal. 28 (2002) 581–590.
[42] S. Agatonovic-Kustrina, J.V. Turnerb, B.D. Glass, J. Pharmaceut. Biomed. Anal. 48 (2008) 369–375.
[43] A. Buciński, A. Socha, M. Wnuk, T. Bączek, A. Nowaczyk, J. Krysiński, K. Goryński, M. Koba, J. Microbiol. Methods 76 (2009) 25–29.